

Meta-Learning Biologically Plausible Plasticity Rules with Random Feedback Pathways

Navid Shervani-Tabar^{*,1} and Robert Rosenbaum¹

¹*Department of Applied and Computational Mathematics and Statistics,
University of Notre Dame, Notre Dame, IN 46556, USA*

**Corresponding author: nshervan@nd.edu*

December 1, 2022

Abstract

Backpropagation is widely used to train artificial neural networks, but its relationship to synaptic plasticity in the brain is unknown. Some biological models of backpropagation rely on feedback projections that are symmetric with feedforward connections, but experiments do not corroborate the existence of such symmetric backward connectivity. Random feedback alignment offers an alternative model in which errors are propagated backward through fixed, random backward connections. This approach successfully trains shallow models, but learns slowly and does not perform well with deeper models or online learning. In this study, we develop a novel meta-plasticity approach to discover interpretable, biologically plausible plasticity rules that improve online learning performance with fixed random feedback connections. The resulting plasticity rules show improved online training of deep models in the low data regime. Our results highlight the potential of meta-plasticity to discover effective, interpretable learning rules satisfying biological constraints.

1 Introduction

Error-driven learning in multilayer neural networks was revolutionized by the error backpropagation algorithm [1], or backprop for short. In backprop, gradients or “errors” are propagated backward through auxiliary feedback pathways to compute parameter updates.

While practical, backprop has strong structural constraints that make it biologically implausible [2, 3]. A major limitation, known as the weight transport problem [4] states that transmitting gradients to upstream layers requires feedback connections that are symmetric with feedforward connections. Such symmetric connectivity is not known to exist in the brain. In an attempt to depart from the symmetry assumption, Lillicrap *et al.* [5] show that even random backward connections can transmit effective teaching signals to train the upstream layers. In this scenario, while the backward connections are fixed, forward weights evolve to align the teaching signals with those prescribed by the backprop algorithm. However, leaving out the

symmetry constraint comes with caveats. Random feedback alignment struggles with deeper networks, limited training data sizes, convolutional layers, and online data streams [6, 7].

To improve random feedback alignment, Nøkland [8] proposed to rewire the feedback connections and feed the teaching signals directly from the output layer to the upstream layers. While this improves the transmission of errors, it still does not perform as robustly as the symmetric case in the low data regime. Parallel to this, Liao *et al.* [9] suggested dismissing symmetry in magnitude, but assigning symmetric signs to the feedback connections. Nonetheless, they found that decreasing the batch size of the training data may deteriorate performance when discarding symmetry. In addition, they found batch normalization [10] critical for training with asymmetric connections. These findings render the methods inadequate for training with an online stream of data, where the batch size is one, and ultimately undercuts their biological plausibility.

An alternative strategy is to implement a secondary update rule to modify the backward connections along with the forward weights. To that end, Akrouf *et al.* [11] proposed to use a Hebbian plasticity rule [12] to adjust the feedback matrices parallel to the approximate gradient-based update of the forward path. The former pushes the backward connections toward the transpose of the forward weights. However, Kunin *et al.* [13] show that this approach is highly sensitive to hyperparameter tuning. Instead, they redefine the optimization objective as a loss function based on the forward path in combination with layer-wise regularization terms for backward weights to update forward and backward pathways concurrently. They propose a few regularization terms and show that combining these units can achieve more stable plasticity rules.

Meta-learning is a broad learning framework consisting of a learning process that envelopes another optimization loop and learns some aspect of the inner learning procedure, effectively “learning to learn.” Although this concept has been around for decades [14], Finn *et al.* [15] popularized meta-learning for few-shot learning applications. This approach employs meta-learning to optimize an internal representation of the network, which is subsequently used as an initial weight to expedite learning on a downstream task. Further, Javed and White [16] extended this approach to continual learning by modifying the objective function of the outer optimization loop. Still, they used the modified approach to learn a partial initialization of the network’s forward weights. Although effective in learning representations for the few-shot learning, they effectively work by pre-training a model rather than by learning to learn. More precisely, their effectiveness is largely derived from their ability to meta-learn a weight initialization, rather than meta-learning a learning rule itself.

The meta-learning framework has provided a new direction for building biologically plausible computational neural models. For example, Lindsey *et al.* [17] learn the direct feedback pathways that modulate activations and use a supervised adaptation of Oja’s rule to update forward connections. It is supervised because it benefits from modulated activations, which do not guarantee the established properties of conventional Oja’s rule [18]. Nevertheless, they also meta-learn an initial value for the forward connections, which makes their approach dependent on the learned weight initialization, not on the learned learning rule alone. Miconi *et al.* [19, 20] showed that meta-plasticity can train a variety of network architectures on various tasks. Like Lindsey *et al.* [17], their approach meta-trains a separate plasticity rule for each weight. While this approach can be effective, the resulting plasticity rules are difficult to interpret. In addition, meta-learning weight initialization in these works makes it unclear to what degree the results are affected by the proposed plasticity rule as opposed to the weight initialization.

A growing body of work aims to only meta-learn a plasticity rule without inferring any component of the inner model such as initial weights. Early work includes Bengio *et al.* [21], who meta-learned a parametric learning rule to train a 2D classifier and boolean function. In each meta-iteration, they used the plasticity rule to train multiple networks on separate tasks and obtained the meta-loss function by summing over the loss of all these networks. More recent work includes Confavreux *et al.* [22], who used meta-plasticity to determine plasticity rules that train shallow linear networks. Rather than discovering new rules, they recover well-known plasticity rules using objective functions based on their known behavior.

Here, we improve upon previous work by discovering a plasticity rule that enhances the flow of information in the backward pathway while learning more distinctive embeddings in the forward network. We use meta-plasticity to learn a parameterized plasticity rule based on a combination of biologically motivated rules. Key features that characterize our approach include:

1. Our approach solely meta-learns a plasticity rule and does not learn a weight initialization. As a result, our approach learns a learning rule that can be applied to train “naive,” randomly initialized networks from scratch.
2. We use “meta-parameter sharing” in the sense that all weights share a common plasticity rule, instead of learning a separate plasticity rule for each weight. This approach allows us to interpret and understand the meta-learned plasticity rules.
3. We impose an $L1$ penalty on the plasticity coefficients in our meta-loss function. This encourages our algorithm to learn a plasticity rule with fewer terms, further simplifying the analysis and interpretability of the resulting rule.
4. Our inner learning loop uses online learning (batch size 1) and limited training data (250 data points). Coupled with the random weight initialization in our inner learning loop, this forces the plasticity rules to learn in a more challenging and biologically relevant setting.

Taken together, we develop a meta-plasticity approach that can derive interpretable plasticity rules satisfying biologically motivated constraints. Our approach further opens the doors to the use of meta-plasticity to understand how effective learning can emerge in biological neural circuits.

2 Results

2.1 Feedback Alignment does not learn effectively in deep networks

Consider a fully-connected deep neural network $f_{\mathbf{W}}$ parameterized by weights \mathbf{W} , representing a non-linear mapping $f_{\mathbf{W}} : \mathbf{x} \mapsto \mathbf{y}_L$ from the network’s input $\mathbf{y}_0 = \mathbf{x}$ to the output \mathbf{y}_L , with L denoting the depth of the network. Each network layer is defined by

$$\mathbf{z}_\ell = \mathbf{W}_{\ell-1,\ell} \mathbf{y}_{\ell-1}, \tag{1}$$

$$\mathbf{y}_\ell = \sigma(\mathbf{z}_\ell), \tag{2}$$

where \mathbf{y}_ℓ is the activation for layer ℓ and σ stands for the non-linear activation function.

Given a dataset $\mathcal{D}_{train} = (\mathbf{X}_{train}, \mathbf{Y}_{train})$, the model is trained in an attempt to find the set of weight parameters $\mathbf{W} = \{\mathbf{W}_{\ell-1,\ell} | 0 < \ell \leq L\}$, that minimize a loss function $\mathcal{L}(\mathbf{y}_L, \mathbf{Y}_{train})$. For instance, in a gradient-based optimization algorithm, the derivative of this loss function with respect to \mathbf{z} is propagated backward up to the initial layer to modulate the weight parameters. A widely used scheme, backprop, relies on an auxiliary symmetric backward network, whose weights $\mathbf{B} = \{\mathbf{B}_{\ell+1,\ell} | 0 < \ell < L\}$ are the transposes of the forward path’s weights, to transport these modulating signals. Backprop employs the chain rule to compute derivatives

$$\mathbf{e}_\ell = \frac{\partial \mathcal{L}}{\partial \mathbf{z}_\ell} = \mathbf{B}_{\ell+1,\ell} \mathbf{e}_{\ell+1} \odot \sigma'(\mathbf{z}_\ell), \quad (3)$$

where \odot denotes element-wise multiplication,

$$\mathbf{e}_L = \frac{\partial \mathcal{L}}{\partial \mathbf{z}_L}, \quad \text{and} \quad \mathbf{B}_{\ell+1,\ell} = \mathbf{W}_{\ell,\ell+1}^T. \quad (4)$$

After deriving the error \mathbf{e}_ℓ , weight parameters are updated by

$$\Delta \mathbf{W}_{\ell-1,\ell} = -\theta \mathbf{e}_\ell \mathbf{y}_{\ell-1}^T, \quad (5)$$

which represents a shared plasticity rule for all forward connections $\mathbf{W}_{\ell-1,\ell}$ and θ is the associated learning rate.

To alleviate the biologically undesirable characteristics of the backprop algorithm, Ref. [5] proposed the ‘‘Random Feedback Alignment’’ approach, which departs from the assumption of symmetric feedback connections in Eq. 4 and instead uses fixed random backward connections $\mathbf{B}_{\ell+1,\ell}$ that are not bound to the forward weights. To distinguish between the two learning algorithms, we hereafter use the phrase ‘‘feedback alignment’’ to refer to the learning rule in Eq. 5 with fixed random $\mathbf{B}_{\ell+1,\ell}$ and we use ‘‘backprop’’ to refer to Eq. 5 with $\mathbf{B}_{\ell+1,\ell} = \mathbf{W}_{\ell,\ell+1}^T$.

For feedback alignment, the teaching signal \mathbf{e}_ℓ^{FA} is not an exact gradient, but an approximating pseudo-gradient term. The resulting learning algorithm performs well on simple tasks and shallower networks. However, feedback alignment fails to reach good accuracy in deeper networks and is not as robust in the small data regime. In our empirical test with an on-line stream of data, feedback alignment and only begins to effectively learn after about 2000 iterations, while backprop learns much more quickly (Fig. 1a). Alternative approaches have proposed a direct feedback pathway [8] from teaching signal \mathbf{e}_L to each layer, but we find that this also does not achieve backprop performance (see Supplementary Fig. S1). In addition, Fig. 1b shows that the teaching signals transmitted through fixed feedback connections \mathbf{e}_ℓ^{FA} are not aligned with the true gradients, \mathbf{e}_ℓ^{BP} , computed by backpropagation at this stage of training.

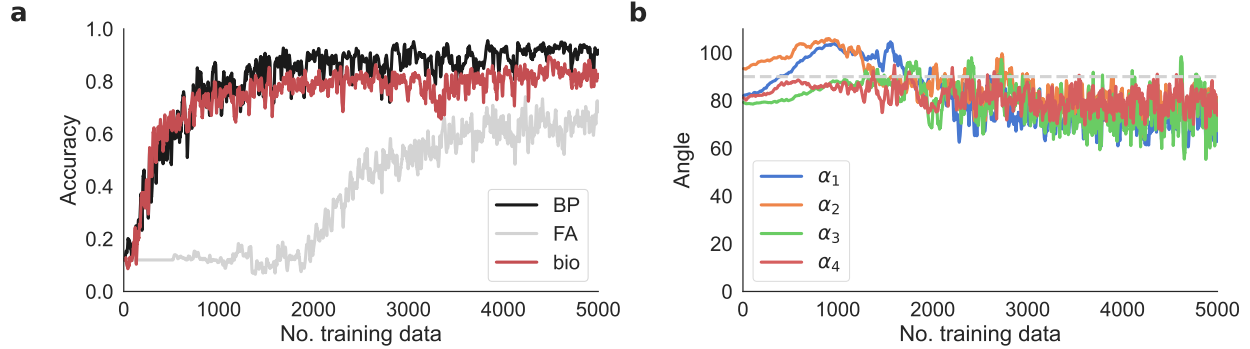


Figure 1: **Feedback alignment learns poorly in deep models:** Performance of benchmark learning schemes while training a 5-layer fully-connected classifier network on MNIST digits [23] with online learning. (a) Accuracy versus the number of training data for Feedback Alignment (FA) [5] and backprop (BP) [1] methods, compared to the discovered biologically inspired plasticity rule (bio) in Sec. 2.2.2. (b) The angle α_ℓ between the teaching signal e_ℓ^{FA} transmitted by the Feedback Alignment method and the corresponding backpropagated signal e_ℓ^{BP} .

These limitations indicate that the backward flow of information through fixed feedback is insufficient for online training in deeper models. This paper investigates modified plasticity rules to improve the trained model’s performance. To that end, a meta-learning framework is adapted to explore a parameterized space of the plasticity rules.

2.2 A meta-plasticity approach for discovering interpretable plasticity rules.

Meta-learning is a machine learning paradigm that aims to learn elements of a learning procedure. Adopting this concept to discover a plasticity rule gives rise to the notion of meta-plasticity. This framework consists of a two-level learning scheme: An inner adaptation loop that learns parameters \mathbf{W} of a model $f_{\mathbf{W}}$ using a parameterized plasticity rule $\mathcal{F}(\Theta)$ and an outer meta-optimization loop that modifies the plasticity meta-parameters Θ . The meta-training dataset contains a set of tasks $\{\mathcal{T}\}$, each consisting of K training data $(\mathbf{X}_{train}, \mathbf{Y}_{train})$ and Q query data $(\mathbf{X}_{query}, \mathbf{Y}_{query})$ per class. The former is used to train the model $f_{\mathbf{W}}$ while the latter optimizes the meta-parameters Θ . Algorithm 1 details the meta-plasticity framework presented in this work.

Algorithm 1 Meta-plasticity algorithm.

Input meta-training set $\{\mathcal{T}\} = \{(\mathbf{X}_{train}, \mathbf{Y}_{train}), (\mathbf{X}_{query}, \mathbf{Y}_{query})\}$, plasticity rule \mathcal{F} , number of episodes \mathcal{E} , meta-learning rate η , and regularization coefficient λ .
Initialize learning parameters $\Theta^{(0)}$.
for $\varepsilon = 0, \dots, \mathcal{E}$ **do**
 Initialize network parameters $\mathbf{W}^{(0)}$ and \mathbf{B} .
 for $(\mathbf{x}_{train}^{(i)}, \mathbf{y}_{train}^{(i)}) \in (\mathbf{X}_{train}, \mathbf{Y}_{train})$ **do**
 Set $\mathbf{y}_0 = \mathbf{x}_{train}^{(i)}$
 for $\ell = 1, \dots, L$ **do**
 Compute \mathbf{z}_ℓ (Eq. 1).
 Compute \mathbf{y}_ℓ (Eq. 2).
 end for
 Compute $\mathcal{L}(\mathbf{y}_L, \mathbf{y}_{train}^{(i)})$.
 Compute \mathbf{e}_L (Eq. 4).
 for $\ell = L, \dots, 1$ **do**
 Compute $\mathbf{e}_{\ell-1} = \mathbf{B}_{\ell, \ell-1} \mathbf{e}_\ell \odot \sigma'(\mathbf{z}_{\ell-1})$ (Eq. 3).
 Update $\mathbf{W}_{\ell-1, \ell}^{(i+1)} = \mathbf{W}_{\ell-1, \ell}^{(i)} + \mathcal{F}(\mathbf{e}_{\ell-1}, \mathbf{y}_{\ell-1}, \mathbf{e}_\ell, \mathbf{y}_\ell, \mathbf{W}_{\ell-1, \ell}^{(i)}; \Theta^{(\varepsilon)})$.
 end for
 end for
 Update meta-parameters $\Theta^{(\varepsilon+1)} = \Theta^{(\varepsilon)} - \eta \nabla_{\Theta^{(\varepsilon)}} \left[\mathcal{L}(f(\mathbf{X}_{query}; \mathbf{W}^{(i+1)}), \mathbf{Y}_{query}) + \lambda \|\Theta^{(\varepsilon)}\|_1 \right]$.
end for

In each meta-iteration, also known as an episode, a randomly initialized model $f_{\mathbf{W}}$ is trained on an online training data sequence. In other words, each adaptation iteration uses a single data point $(\mathbf{x}_{train}, \mathbf{y}_{train})$ to update \mathbf{W} . It is worth emphasizing that reinitializing weights \mathbf{W} at each episode removes the learning rule’s dependence on the weight initialization. The meta-learned plasticity rules are therefore optimized to learn a task starting from a randomly initialized weight matrix. In contrast, meta-optimizing initial weights will adapt meta-parameters Θ to the later stages of learning, which does not extrapolate to the training lifetime anymore. Moreover, when meta-learning a weight initialization in conjunction with a plasticity rule, it is not clear to what extent improvements in learning can be attributed to the weight initialization versus the meta-learned plasticity rule itself.

Each episode ε follows two objectives. The first is to quantify and update the model parameters \mathbf{W} using a loss function \mathcal{L} , iteratively, on each data point sampled from task $\mathcal{T}^{(\varepsilon)}$ ’s training set. The second objective, dubbed meta-loss, assesses the meta-parameters Θ by evaluating the loss function \mathcal{L} on the query set of the same task $\mathcal{T}^{(\varepsilon)}$ using the updated model $f_{\mathbf{W}}$. Mathematically put,

$$\mathcal{L}_{meta} = \mathcal{L}(f_{\mathbf{W}}(\mathbf{X}_{query}), \mathbf{Y}_{query}) + \lambda \|\Theta\|_1, \quad (6)$$

where $f_{\mathbf{W}}$ is the model updated in the adaptation loop and λ is a predefined hyperparameter. The regularization term in Eq. 6 is the $L1$ norm of the meta-parameters, leading the algorithm to favor simplicity in the plasticity model. While weights \mathbf{W} are optimized using $\mathcal{F}(\Theta)$, meta-parameters Θ are updated by a gradient-based approach. Figure 2 summarizes the problem’s configuration.

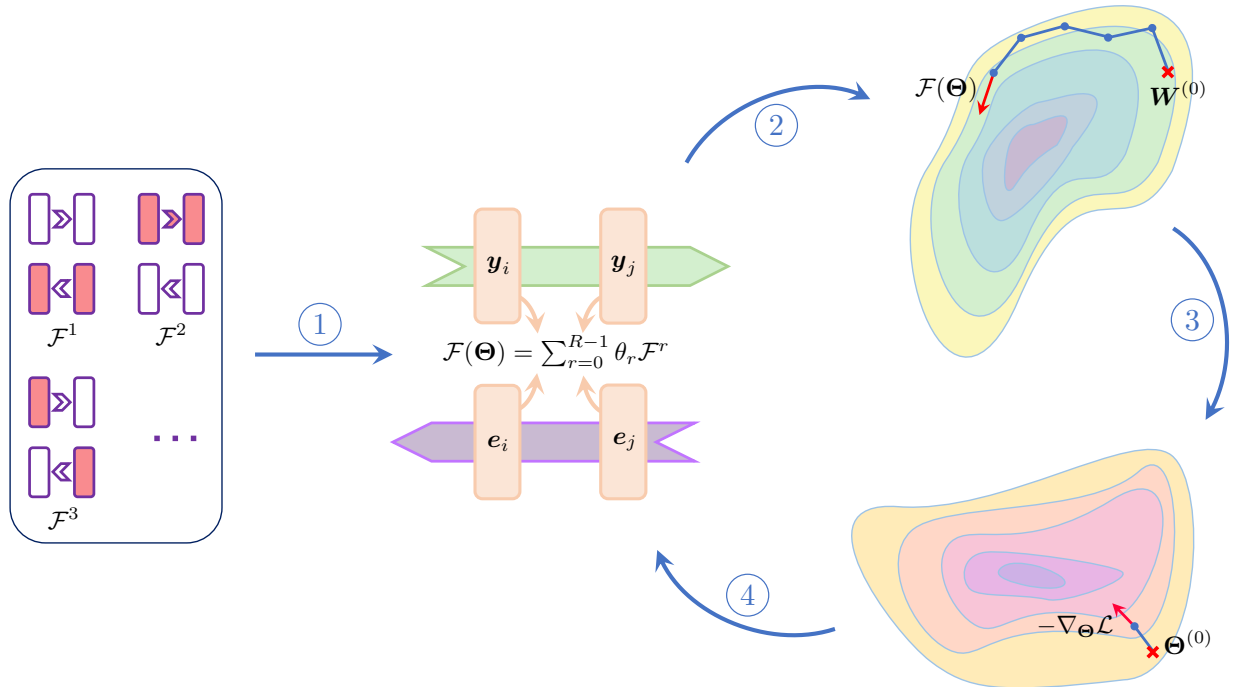


Figure 2: **Schematic depiction of the meta-plasticity workflow:** (1) A pool of R biologically motivated plasticity terms $\{\mathcal{F}^r\}_{0 \leq r \leq R-1}$ is exploited to define a plasticity rule $\mathcal{F}(\Theta)$ that governs the weight updates of the model $f_{\mathbf{W}}$. Each term \mathcal{F}^r integrates local elements available to the weight, including pre-synaptic activation \mathbf{y}_i , post-synaptic activation \mathbf{y}_j , pre-synaptic error \mathbf{e}_i , post-synaptic error \mathbf{e}_j , and the current state of the weight $\mathbf{W}_{i,j}$. The linear combination of these terms defines plasticity rule $\mathcal{F}(\Theta)$, where $\Theta = \{\theta_r | 0 \leq r \leq R-1\}$ is the set of meta-parameters shared across the network. (2) The parameterized local learning rule $\mathcal{F}(\Theta)$ is used to navigate the weight parameter space. At each episode ε , $\mathcal{F}(\Theta^{(\varepsilon)})$ iteratively searches for optimized \mathbf{W} starting from a random weight $\mathbf{W}^{(0)}$. A single data point sampled from $\mathcal{T}^{(\varepsilon)}$'s train set is used at each adaptation step for online training of the model. (3) In the meta-optimization phase, the solution \mathbf{W} of the inner loop is used to compute the loss on the query set of task $\mathcal{T}^{(\varepsilon)}$. Then, a gradient-based strategy explores the meta-parameter space to optimize the plasticity meta-parameters $\Theta^{(\varepsilon)}$. (4) The plasticity rule $\mathcal{F}(\Theta)$ is reconstructed using the updated meta-parameters $\Theta^{(\varepsilon+1)}$ to guide the weight optimization in the next episode. This procedure is repeated until the meta-parameters converge. In the initial episodes, the unoptimized $\mathcal{F}(\Theta)$ is unlikely to direct \mathbf{W} to a solution. However, as Θ converges, $\mathcal{F}(\Theta)$ discovers a new direction that may only partially adhere to the direction of the gradient.

2.2.1 Meta-learning the learning coefficients via backprop and feedback alignment establishes a benchmark

Before introducing new plasticity rules, it is necessary to establish the baseline performance for the current learning models for the learning task considered here. To this end, we use the meta-plasticity framework to optimize the learning rate, θ , in Eq. 5 for backprop and feedback alignment. Since, in these examples, the meta-plasticity model seeks to optimize the meta-parameter rather than selecting one term over the other, the regularization coefficient λ in Eq. 6 is set to zero.

Figures 3a - 3c compare the performance of the two plasticity rules over 500 episodes. First, the reinitialized models $f_{\mathbf{W}}$ are trained at each episode using an online stream of $M \times K = 250$ data points. Then, the meta-accuracy and meta-loss are evaluated with the query data. Tracing the evolution of the plasticity coefficients in Fig. 3c shows that the meta-plasticity model

converges after ~ 100 episodes. After convergence, the model trained with feedback alignment is, on average, about 25% accurate in its predictions, whereas the model backpropagated via symmetric feedbacks reaches an approximate accuracy of about 70%. The comparison shows that the former is not adequately trained with an online data stream in the small data regime. This outcome is further supported by Fig. 3d, which illustrates the poor alignment of the modulating signals in feedback alignment with the backprop analogs.

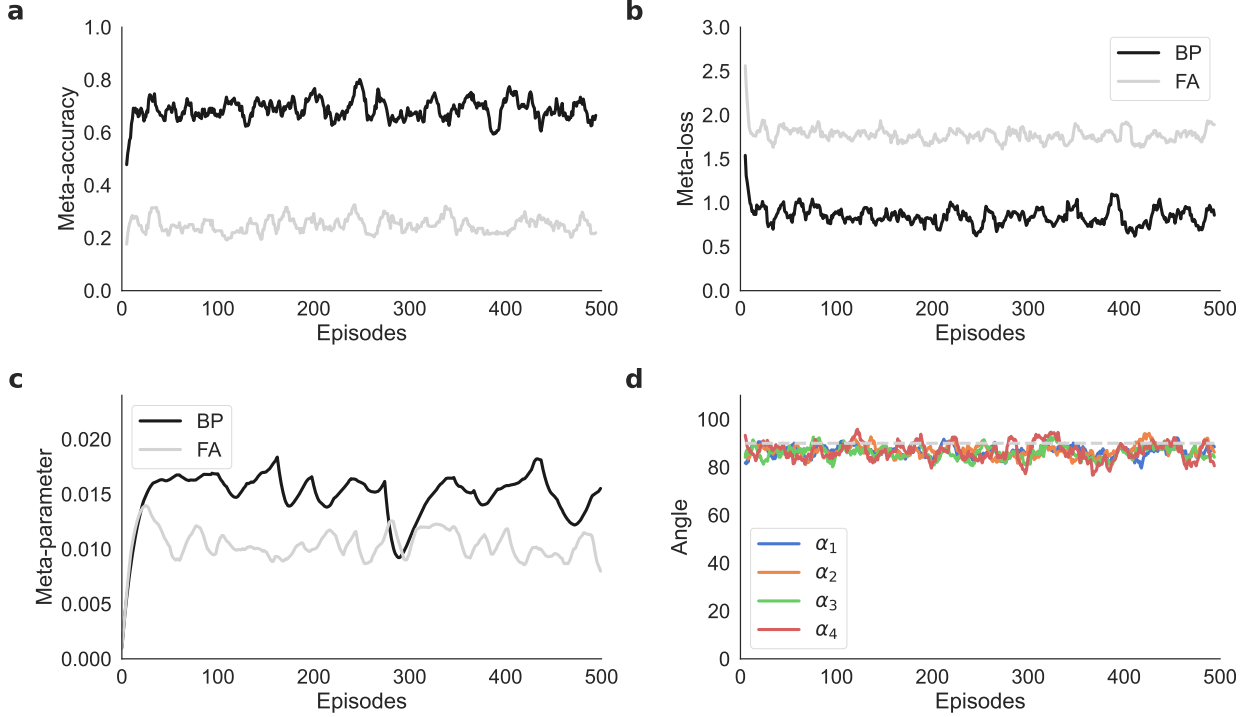


Figure 3: **Meta-learning coefficients for feedback alignment and backprop.** (a) Meta-accuracy of feedback alignment (FA) compared to backprop (BP) trained using the meta-plasticity framework (Alg. 1) during 500 meta-optimization episodes and (b) the corresponding meta-loss, (c) evolution of the learning rate meta-parameter (initialized to 10^{-3}) with feedback alignment (FA) compared to backprop (BP) during 500 meta-optimization episodes. In this figure, each meta-parameter was optimized separately in a single-parameter meta-optimization problem and is superimposed for comparison. (e) Alignment angle α_ℓ between modulating signals of the feedback alignment e_ℓ^{FA} and backprop e_ℓ^{BP} for $l = 1, 2, 3$, and 4. For both approaches, e_5 is computed using Eq. 4 and has the same value, resulting in $\alpha_5 = 0$. All loss, accuracy, and alignment results here and in the figures below are plotted with a moving average window of 11 data points.

2.2.2 Biologically inspired plasticity rules

The analysis in section 2.2.1 indicated a substantial performance gap between the backprop model and the pseudo-gradient rule with random feedback pathways early in the learning process. However, with the interrupted backward flow as the only distinction between the two rules, the error in the last layer and activations still maintain proper information. Intuitively, introducing new local combinations of these terms to the plasticity rule may restore information flow and improve performance. To that end, we define a set of candidate plasticity terms and use meta-plasticity to uncover combinations that enhance learning. Meta-plasticity helps in two ways: finding the optimized set of meta-parameters for the linear combination of candidate terms and selecting the dominant plasticity terms. While the former avoids cumbersome

hand-tuning of the coefficients, the latter provides a tool for systematically studying the space of learning rules.

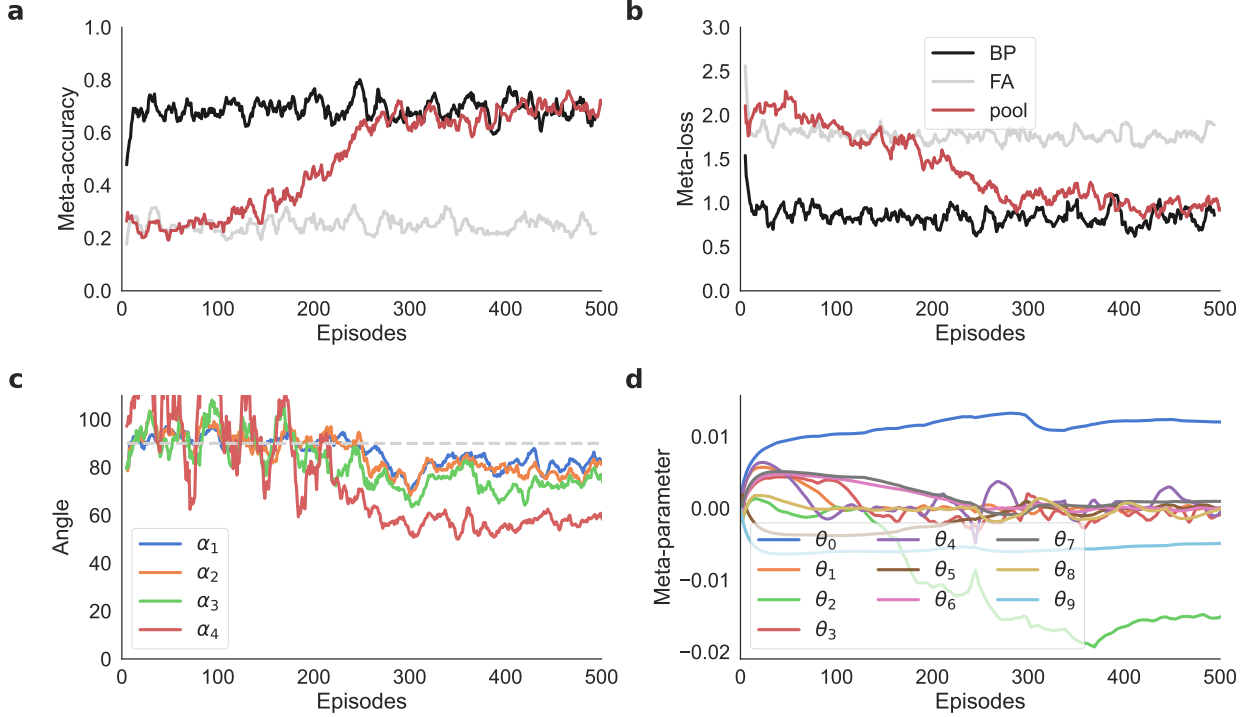


Figure 4: **Performance of the model trained with the pool of biologically inspired plasticity rules \mathcal{F}^{pool} :** (a) Accuracy and (b) loss for \mathcal{F}^{pool} compared to \mathcal{F}^0 via feedback alignment (FA) and backprop (BP), (c) alignment of the teaching signals of \mathcal{F}^{pool} with the ones for backprop, and (d) convergence of the plasticity coefficients.

Given a set of R candidate terms $\{\mathcal{F}^r\}_{0 \leq r \leq R-1}$, the plasticity rule optimized by the meta-plasticity algorithm is defined as

$$\mathcal{F}^{pool}(\Theta) = \sum_{r=0}^{R-1} \theta_r \mathcal{F}^r.$$

We began by considering a pool of $R = 10$ plasticity terms (see Methods for details). While meta-learning over the query set of sampled tasks for this pool of plasticity terms yields an optimized set of meta-parameters, Θ , the resulting plasticity rule consists of too many terms which are difficult to interpret and understand and whose underlying mechanisms may overlap. Therefore, following Occam’s razor, we included an $L1$ penalty on plasticity coefficients to select for a sparser set of plasticity terms (see Eq. 6). Figure 4a–c illustrates the performance of the model. Figure 4d shows that the coefficients for all but 3 terms converge toward zero after about 300 episodes. Those three terms are a pseudo-gradient rule (\mathcal{F}^0), a Hebbian-like plasticity rule (\mathcal{F}^2), and Oja’s rule (\mathcal{F}^9 ; see Methods and below for definitions of these rules).

Selecting these three terms and omitting the others gives a simpler plasticity rule of the form

$$\begin{aligned} \mathcal{F}^{bio}(\Theta) = & -\theta_0 \mathbf{e}_\ell \mathbf{y}_{\ell-1}^T \\ & -\theta_2 \mathbf{e}_\ell \mathbf{e}_{\ell-1}^T \\ & -\theta_9 (\mathbf{y}_\ell \mathbf{y}_{\ell-1}^T - (\mathbf{y}_\ell \mathbf{y}_\ell^T) \mathbf{W}_{\ell-1, \ell}), \end{aligned} \quad (7)$$

where $\Theta = \{\theta_0, \theta_2, \theta_9\}$ is the set of plasticity meta-parameters. \mathcal{F}^{bio} performs similar to the \mathcal{F}^{pool} (see Supplementary Fig. S2) and significantly improves the performance of the feedback alignment method in the low data regime (Fig. 1).

While the meta-plasticity successfully discovers \mathcal{F}^{bio} , it is important to interpret the plasticity rule and understand how it leads to improved learning. \mathcal{F}^{bio} consists of three components: a pseudo-gradient term, a Hebbian-style error term, and Oja’s rule. In what follows, we study the latter terms separately with the pseudo-gradient term to unveil the underlying reason behind their performance.

Hebbian-style error term

Motivated to understand the Hebbian-style error-based learning term in Eq. 7, we rerun the model using a plasticity rule that only includes the modified Hebbian term and the pseudo-gradient term, but omits the third term

$$\mathcal{F}^{eHebb}(\Theta) = -\theta_0 \mathbf{e}_\ell \mathbf{y}_{\ell-1}^T - \theta_2 \mathbf{e}_\ell \mathbf{e}_{\ell-1}^T. \quad (8)$$

In Fig. 5, the meta-plasticity algorithm is used to optimize the coefficients θ_0 and θ_2 , which are initialized to 10^{-3} and zero, respectively. Comparing the accuracy and the loss plot to \mathcal{F}^{bio} ’s performance (Fig. S2) shows that while \mathcal{F}^{eHebb} demonstrates a significant improvement over \mathcal{F}^0 via feedback alignment, it is yet to reach that of \mathcal{F}^{bio} . Despite this, the alignment angles of \mathcal{F}^{eHebb} (Fig. S2) are superior to \mathcal{F}^{bio} ’s, which indicates that the Hebbian error term is the driving force behind aligning the teaching signals in \mathcal{F}^{bio} .

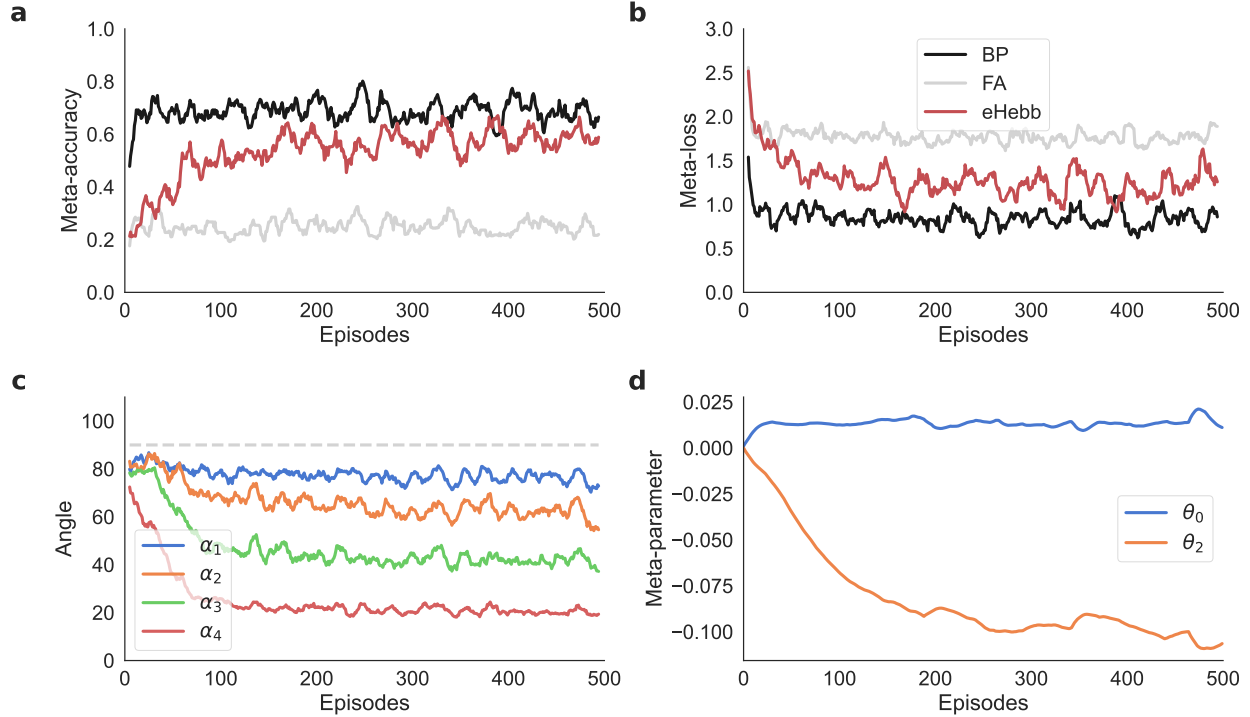


Figure 5: **Performance of the image classification network trained with \mathcal{F}^{eHebb} (Eq. 8):** (a) Meta-accuracy and (b) meta-loss plots for \mathcal{F}^{eHebb} compared to \mathcal{F}^0 via feedback alignment (FA) and backprop (BP), (c) alignment angles for modulating signals across the network, and (d) convergence of the plasticity coefficients using the meta-plasticity model.

Figure 6 illustrates how \mathcal{F}^{eHebb} alters the communications between the backward and forward pathways. The diagram on the left in Fig. 6a shows a model solely trained with the \mathcal{F}^0 via feedback alignment. In this scenario, the information from $\mathbf{B}_{2,1}$ flows to $\mathbf{W}_{0,1}$ through Eq. 3, which is then propagated to $\mathbf{W}_{1,2}$ during the forward pass. This configuration updates $\mathbf{W}_{1,2}$ to align the modulator vector \mathbf{e}_1 with the backprop counterpart. Nonetheless, this machinery does not sufficiently align the modulating signals when applied to deeper networks with fewer training iterations. In the diagram on the right, the last layer is updated with an additional Hebbian-style plasticity term \mathcal{F}^2 , while the first layer is trained with vanilla \mathcal{F}^0 rule via feedback alignment. Once again, information from $\mathbf{B}_{2,1}$ flows into $\mathbf{W}_{0,1}$. However, this time, \mathcal{F}^{eHebb} introduces an auxiliary channel to flow the information from $\mathbf{B}_{2,1}$ to $\mathbf{W}_{1,2}$. Finally, the forward propagation through the network implicitly transmits the information from $\mathbf{B}_{2,1}$ to $\mathbf{W}_{1,2}$. The modified rule \mathcal{F}^{eHebb} establishes an explicit supplementary means to communicate between $\mathbf{B}_{2,1}$ and $\mathbf{W}_{1,2}$, boosts the alignment of \mathbf{e}_1 , and improves the model’s performance.

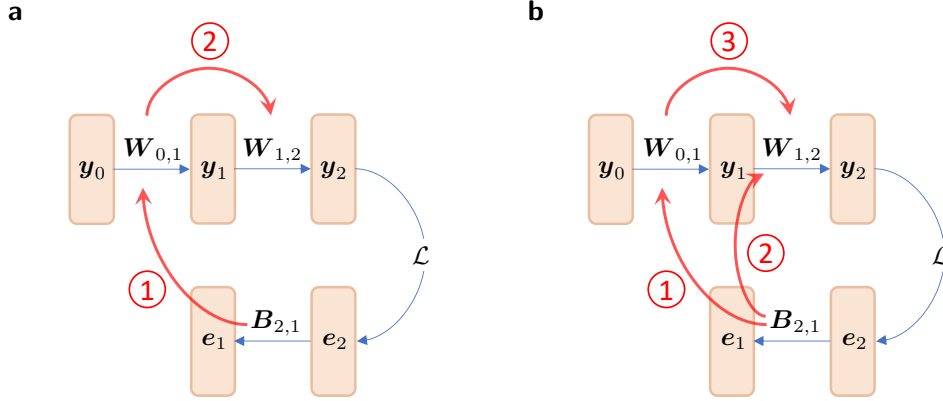


Figure 6: **Information flow between the forward and backward pathways:** (a) Both layers are trained with \mathcal{F}^0 rule via feedback alignment. (b) The first layer is updated with \mathcal{F}^0 rule via feedback alignment, while the second layer uses \mathcal{F}^{eHebb} . The blue arrows depict information propagation through the forward and backward paths. The communications between feedback and feedforward pathways are represented with red arrows.

To corroborate the argument above, we consider a 3-layer network trained with \mathcal{F}^0 rule via feedback alignment and inspect the effect of adding \mathcal{F}^{eHebb} on the alignment angles in different layers. To that end, rather than sharing the same learning rule across the network, each layer is updated using one of the \mathcal{F}^0 rule via feedback alignment or \mathcal{F}^{eHebb} rules. Table 1 determines that adding the Hebbian error term to the weight update reduces the alignment angle between the pre-synaptic error and its backprop analog. A more detailed discussion can be found in Supplementary Notes.

\mathcal{F}^0	\mathcal{F}^{eHebb}	α_0	α_1	α_2
$W_{0,1}, W_{1,2}, W_{2,3}$	-	89.89	76.69	82.04
$W_{0,1}, W_{2,3}$	$W_{1,2}$	89.95	59.95	72.14
$W_{0,1}, W_{1,2}$	$W_{2,3}$	90.03	75.18	29.02
$W_{2,3}$	$W_{0,1}, W_{1,2}$	75.29	61.23	72.56
$W_{0,1}$	$W_{1,2}, W_{2,3}$	90.2	49.4	27.9
$W_{1,2}$	$W_{0,1}, W_{2,3}$	84.86	74.25	30.33
-	$W_{0,1}, W_{1,2}, W_{2,3}$	77.93	49.93	28.4

Table 1: **Effect of the Hebbian-like error learning rule \mathcal{F}^{eHebb} on the alignment of the modulating signals α_ℓ for different layers:** The leftmost column includes the parameters updated using \mathcal{F}^0 with feedback alignment, and the next column indicates layers trained with \mathcal{F}^{eHebb} (Eq. 8). Angles α_ℓ are presented in degrees. Since e_0 is a synthetic error, the effect of the \mathcal{F}^{eHebb} on $W_{0,1}$ alone has been excluded. The model is trained for 500 episodes, and the computed angles are averaged after a burn-in period of 100 episodes.

For a more precise, mathematical intuition of the effects that \mathcal{F}^{eHebb} has on weights, we show in Supplementary Notes that, in a linear network model under reasonable approximating assumptions,

$$\mathbb{E} [e_\ell e_{\ell-1}^T \mid B_{\ell,\ell-1}] \propto B_{\ell,\ell-1}^T$$

for layers, $\ell = 1, 2, \dots, L - 1$. Thus, the term $e_\ell^T e_{\ell-1}$ in \mathcal{F}^{eHebb} pushes $W_{\ell-1,\ell}$ toward the

transpose of $\mathbf{B}_{\ell,\ell-1}$, resulting in faster alignment of the modulatory signals with the backprop algorithm’s error vectors and more efficient learning.

Oja’s rule

Eq. 7 proposes a plasticity rule to train deep networks using fixed feedback matrices. Above, we demonstrated that the Hebbian-style learning term improves the trained model’s performance by improving the modulatory signals’ alignments with the backpropagated analogs. Here, we look at the remaining plasticity term in Eq. 7: Oja’s rule, a purely local learning rule that updates the weights based on its current state and the local activations in the forward path. To this end, we redefine the plasticity rule as a linear combination of the pseudo-gradient term and Oja’s rule

$$\mathcal{F}^{Oja}(\Theta) = -\theta_0 \mathbf{e}_\ell \mathbf{y}_{\ell-1}^T - \theta_9 (\mathbf{y}_\ell \mathbf{y}_{\ell-1}^T - (\mathbf{y}_\ell \mathbf{y}_\ell^T) \mathbf{W}_{\ell-1,\ell}). \quad (9)$$

We initialize θ_0 to 10^{-3} and θ_9 to zero and employ Alg. 1 to optimize the set of meta-parameters Θ . Figures 7a and 7b illustrate that adding Oja’s rule to the pseudo-gradient term enhances the model’s accuracy when backward connections are fixed. Figure 7c presents the angles between the teaching signals ensued by Eq. 9 and the corresponding backpropagated ones. While the accuracy and loss are significantly improved, contrary to expectations, Oja’s rule does not substantially reduce the alignment angles (Fig. 7c, compare to Figs. 3d and Fig. 5c).

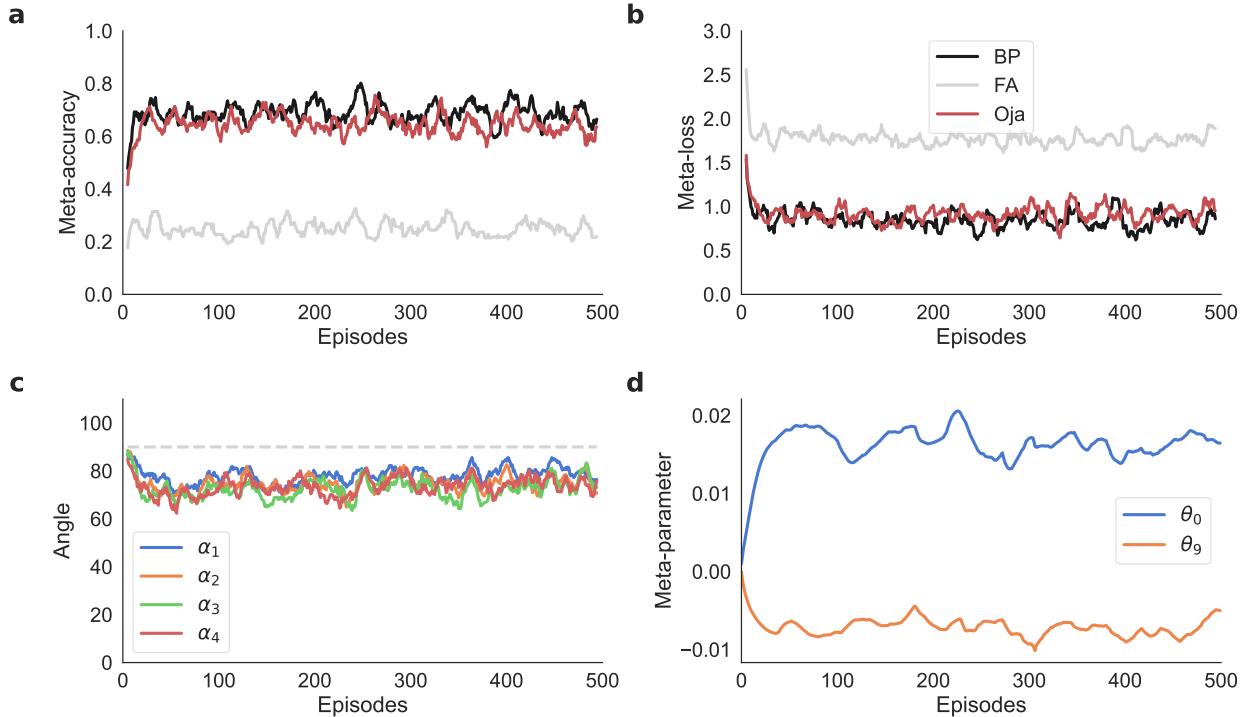


Figure 7: **Performance of the model trained using \mathcal{F}^{Oja} (Eq. 9) through fixed backward connections:** (a) Meta-accuracy and (b) meta-loss of \mathcal{F}^{Oja} compared to \mathcal{F}^0 learning rule via feedback alignment (FA) and backprop (BP), (c) alignment of modulating signals of \mathcal{F}^{Oja} with backprop’s teaching signals, and (d) evolution of the plasticity meta-parameters.

Rather than helping to align the modulating signals, Oja’s rule helps by entirely circumventing the backward path. Instead, it implements a recursive non-linear Principal Component Analysis algorithm, PCA, [24, 25] and thus, extracts feature maps in the forward path through unsupervised learning. For an incoming data stream, Oja’s rule implements a Hebbian learning rule subjected to an orthonormality constraint on the weights. Studying the convergence of this plasticity term reveals that [26] for a compression layer, where $\dim(\mathbf{y}_{\ell-1}) > \dim(\mathbf{y}_\ell)$, rows of the weight matrix $(\mathbf{W}_{\ell-1,\ell})_1, \dots, (\mathbf{W}_{\ell-1,\ell})_{\dim(\mathbf{y}_\ell)}$ will tend to a rotated basis in the $\dim(\mathbf{y}_\ell)$ -dimensional subspace spanned by the principal directions of the input $\mathbf{y}_{\ell-1}$.

By analyzing the continuous-time differential equation corresponding to the Oja’s learning rule, Williams [26] and Oja [25] establish the stability limits for this rule. In a compression layer, the fixed point of Oja’s rule is a stable solution if $\mathbf{W}_{\ell-1,\ell} \mathbf{W}_{\ell-1,\ell}^T = \mathbf{I}$. This conclusion can be used to derive a proximity measure [27, 28, 29] of the estimated $\mathbf{W}_{\ell-1,\ell}$ to a stable solution of Oja’s rule in the presence of non-linear activations. The error

$$E_W = \|\mathbf{z}_\ell - \mathbf{W}_{\ell-1,\ell} \bar{\mathbf{y}}_{\ell-1}\|_2^2, \tag{10}$$

where

$$\bar{\mathbf{y}}_{\ell-1} = \mathbf{W}_{\ell-1,\ell}^T \sigma(\mathbf{z}_\ell),$$

can define this measure. Figure 8 studies this orthonormality measure in models trained with different plasticity rules. Results show that using Oja’s rule will render the weight matrices increasingly orthonormal, reducing the correlation in weight rows and improving the feature extraction in these layers. It is noteworthy that such an unsupervised scheme is not appropriate for training the last layer, which connects the hidden layers to the output. However, doing so, we did not observe a deteriorated performance. Hence for the sake of generality, we share the same plasticity rule across the network. Ultimately, rather than improving the alignments, Oja’s rule provides embeddings that facilitate more effective learning in the last layer.

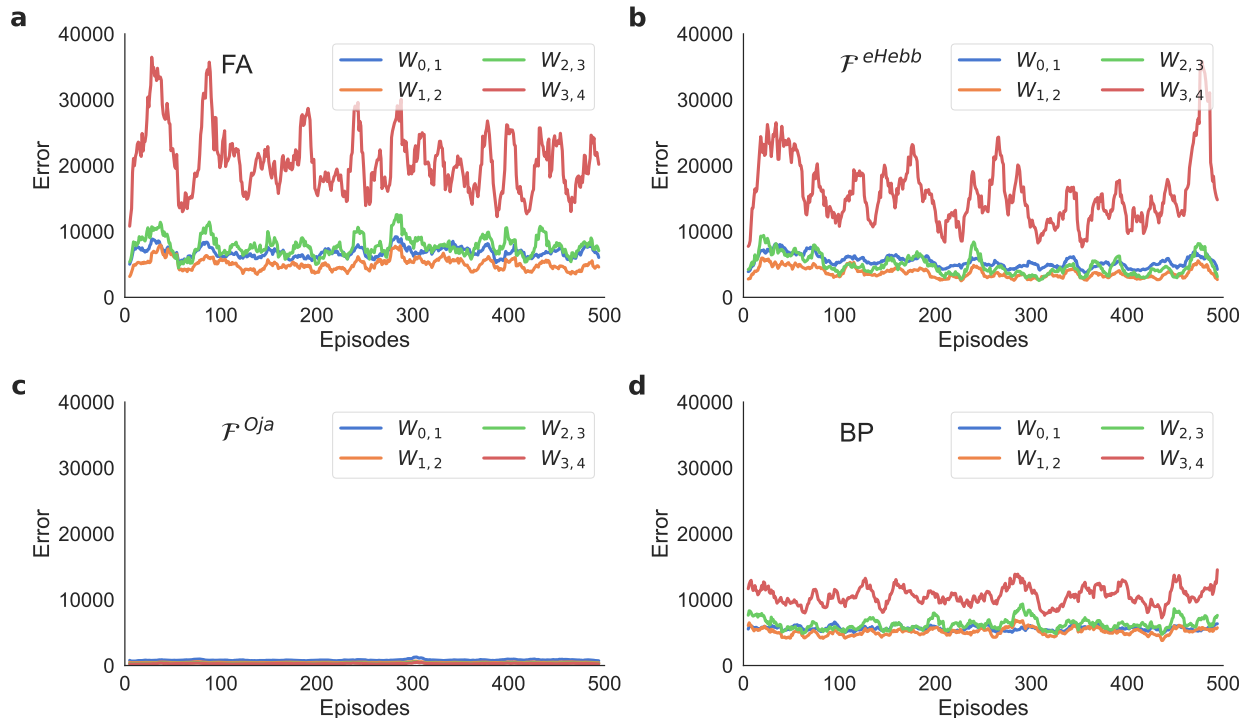


Figure 8: **Orthonormality error through a deep network for different plasticity rules:** Orthonormality errors are measured by Eq. 10 for different layers of a 5-layer deep network. The model is trained using (a) \mathcal{F}^0 via feedback alignment (FA), (b) \mathcal{F}^{eHebb} , (c) \mathcal{F}^{Oja} , and (d) backprop (BP). In this comparison, the last layer has been excluded.

3 Discussion

Despite the dominance of the backpropagation algorithm as the primary technique to train deep neural networks, its biological plausibility remains a significant ground for contest [2, 3]. In particular, the presence of feedback synaptic projections that are precisely symmetric to the forward projections is not biologically realistic. Previous work [5] showed that learning can be achieved without this symmetry using feedback connections that are randomly sampled, not tied to the forward path, and fixed throughout the training process. While a breakthrough, this method is susceptible to diminished performance when training deeper networks or using smaller batch sizes [6, 7]. The latter is a challenge for online learning.

A recent body of work attempts to improve learning through asymmetric feedback connections. They either rewire fixed feedback connections, use plastic feedback connections that are updated through an auxiliary plasticity rule, or impose partial symmetry in the backward network [8, 17, 20, 19, 9]. Our work accelerates learning by improving plasticity rules while transmitting teaching signals through fixed connections. The proposed plasticity rules draw upon biological learning rules, including Hebbian plasticity and Oja’s rule, to combine information locally from their immediate neighbors, including pre- and post-synaptic activations and the corresponding errors. A linear combination of these terms yields a parameterized learning rule. To overcome the arduous hand-tuning of these hyper-parameters, we use a meta-plasticity approach that systematically explores the pool of candidate plasticity rules. This approach consists of an inner loop that learns a task and an outer loop that updates the plasticity coefficients.

The inner loop always starts from randomly initialized weights, so the model must learn to learn from scratch. Moreover, the inner loop learns from an online stream of training data, simulating real-time learning in the brain.

Using this meta-plasticity approach, we discover two plasticity rules that accelerate learning through fixed feedbacks. The first one uses a Hebbian-style learning term to feed a combination of the neighboring modulating signals to the forward path. The second one is Oja’s rule [18], which uses pre- and post-synaptic activations and the current state of their connection to update weights. We investigated each plasticity rule, its underlying mechanism, and how it contributes to learning, revealing two distinct mechanisms behind them. First, the Hebbian-like error term improves performance by modifying the flow of information through the backward path. It introduces an auxiliary channel to communicate information about the backward connections to the forward weights. As a result, it accelerates learning by better aligning modulating signals with the ones transmitted through a symmetric feedback connection. Ultimately, the modified plasticity alters the training to resemble backpropagation. Unlike the Hebbian-like rule, Oja’s rule does not directly affect the flow of the feedback signals. Instead, it acts only on the forward path, implementing an unsupervised learning scheme that extracts feature maps independently of the labels and loss. The updated weight rows approximate an orthonormal basis in the subspace spanned by PCA eigenvectors of the pre-synaptic activations [25]. The strengthened signal separation capabilities in the earlier layers improve predictions made by the output layer.

As the first mechanism tends to align modulating signals with the symmetric counterparts, its performance may at best match that of backprop. However, as Oja’s rule does not aim to imitate backprop, its performance is not bounded by that of backprop, and hence it can also be used to enhance learning in symmetric feedback models. For instance, we realized that adding Oja’s plasticity rule to the gradient-based learning term accelerates learning for poorly initialized networks. This observation explains why the improved performance in the fixed feedback model may outperform learning in the symmetric case. A similar concept was used in the earlier works to initialize internal representations of the neural networks [29]. However, that work used weights preprocessed by Oja’s rule to start gradient-based learning rather than using both terms simultaneously as the plasticity rule. Hence, our results demonstrate the utility of the proposed meta-plasticity approach as a tool for combining different learning terms as a single parameterized learning rule.

We applied our meta-learning approach specifically to overcome the difficulties of learning with fixed feedback connections, but the approach can be applied more widely to discover interpretable learning rules satisfying biological constraints in a variety of contexts and models. For example, we only considered plasticity in the forward connections, but the same approach could be used to learn plasticity rules for backward connections as well. Another interesting future direction is to meta-learn the *architecture* of the feedback pathways instead of (or in addition to) the plasticity parameters. That is, to simultaneously provide both direct [8] and regular [5] feedback pathways and allow the meta-learning algorithm to pick the most efficient path to carry the teaching signals to each layer.

In another direction, our meta-parameter sharing approach could be partially relaxed without learning a new plasticity rule for each connection. For example, one could consider a network with several neural populations and a shared plasticity rule for each pair of populations. This approach could help understand the role of distinct neuron types and populations in biological circuits.

We focused on meta-learning biologically motivated plasticity rules, but our approach can

also be applied to discover learning rules that satisfy other constraints or optimize other meta-loss functions. For example, the approach can be used to find learning rules that can be implemented in non-standard hardware like neuromorphic chips or optical networks, or to discover learning rules that minimize energy consumption or other factors.

In summary, we developed and tested a meta-plasticity approach designed to produce simple, interpretable plasticity rules that can effectively learn on new data. First, using randomly initialized weights on each iteration of the outer loop (instead of meta-learning the initialization) and using online learning in our inner loop encouraged plasticity rules that can perform online learning from scratch. Secondly, meta-parameter sharing yielded a vastly smaller set of learned plasticity rules compared to learning a plasticity rule for each synapse. Finally, an L1 penalty on plasticity coefficients promoted sparsity within the learning rule, ultimately yielding a small set of plasticity terms that are more readily interpreted. Our results demonstrate the utility of this approach for discovering and interpreting plasticity rules. Taken together, our work opens new avenues to the application of meta-plasticity for discovering interpretable plasticity rules that satisfy biological or other constraints.

4 Methods

4.1 Models

Figure 1 performs a 10-way classification on the MNIST dataset, with images resized to 28×28 dimensions. The model is a 5-layer fully connected neural network with dimensions 784-170-130-100-70-47. Hidden layers use the softplus activation function

$$\sigma(\mathbf{z}_\ell) = \frac{1}{\beta} \log(1 + \exp(\beta \mathbf{z}_\ell)), \quad (11)$$

with $\beta = 10$. The output layer uses the softmax activation function. Figures 3 - 5 and 7 - 8 perform 5-way classification on the EMNIST dataset. These figures use the same architecture as Fig. 1. For Tab. 1, the model conducts a 5-way classification on the EMNIST dataset with an image size of 28×28 . The model is a 3-layer fully connected neural network with dimensions 784-130-70-47. Like the rest of the paper, hidden layers use softplus non-linearity with $\beta = 10$, while the output layer uses softmax.

For the fixed feedback pathway problem, feedback connections and weights are initialized to random values that are not equal. For both symmetric and fixed feedback models, connections are reinitialized using the Xavier method [30] at the beginning of each meta-learning episode.

In Figs. 4, 5, 7, and 8, and Tab. 1, we set the initial value for the learning rate θ_0 of the term \mathcal{F}^0 to 10^{-3} and set all other hyper-parameters to zero.

4.2 Candidate learning terms

Section 2.2.2 presented a plasticity rule that improves the model’s performance in the presence of fixed random feedback connections (Eq. 7). We employed the meta-plasticity framework described in section 2.2 to explore a set of local learning rules to discover such a plasticity term. This set of terms is defined as

$$\begin{aligned} \mathcal{F}^0 &= -\theta_0 \mathbf{e}_\ell \mathbf{y}_{\ell-1}^T, \\ \mathcal{F}^1 &= -\theta_1 \mathbf{y}_\ell \mathbf{e}_{\ell-1}^T, \\ \mathcal{F}^2 &= -\theta_2 \mathbf{e}_\ell \mathbf{e}_{\ell-1}^T, \\ \mathcal{F}^3 &= -\theta_3 \mathbf{W}_{\ell-1, \ell}, \\ \mathcal{F}^4 &= -\theta_4 \mathbf{1}_\ell \mathbf{e}_{\ell-1}^T, \\ \mathcal{F}^5 &= -\theta_5 \mathbf{e}_\ell \mathbf{1}_\ell^T \mathbf{y}_\ell \mathbf{y}_{\ell-1}^T, \\ \mathcal{F}^6 &= -\theta_6 \mathbf{y}_\ell \mathbf{y}_\ell^T \mathbf{W}_{\ell-1, \ell} \mathbf{e}_{\ell-1} \mathbf{e}_{\ell-1}^T, \\ \mathcal{F}^7 &= -\theta_7 \mathbf{e}_\ell \mathbf{y}_\ell^T \mathbf{W}_{\ell-1, \ell} \mathbf{e}_{\ell-1} \mathbf{y}_{\ell-1}^T, \\ \mathcal{F}^8 &= -\theta_8 \mathbf{y}_\ell \mathbf{y}_{\ell-1}^T \mathbf{W}_{\ell-1, \ell}^T \mathbf{e}_\ell \mathbf{e}_{\ell-1}^T, \\ \mathcal{F}^9 &= -\theta_9 (\mathbf{y}_\ell \mathbf{y}_{\ell-1}^T - (\mathbf{y}_\ell \mathbf{y}_\ell^T) \mathbf{W}_{\ell-1, \ell}). \end{aligned}$$

Computing the learning terms \mathcal{F}^1 , \mathcal{F}^2 , \mathcal{F}^4 , \mathcal{F}^6 , \mathcal{F}^7 , and \mathcal{F}^8 requires a pre-synaptic error term. In order to update the weights in the first layer $\mathbf{W}_{0,1}$, where there is no pre-synaptic error, we define a synthetic error \mathbf{e}_0 using Eq. 3 and the activation function in Eq. 11, such that

$$\mathbf{e}_0 := \mathbf{B}_{1,0} \mathbf{e}_1 \odot (1 - \exp(-\beta \mathbf{y}_0)).$$

4.3 Meta-Training

Section 2.2 presented a meta-plasticity framework for swiftly exploring a pool of plasticity terms and uncovering combinations that exceed the performance of the existing plasticity rule. We demonstrate this by training a classifier network, which performs a 5-way classification on 28×28 images. The cross-entropy function evaluates the loss in the adaptation loop, whereas the meta-loss is determined by Eq. 6. While, in principle, any optimization algorithm, such as evolutionary methods, can be used to optimize Θ , the algorithm presented in Alg. 1 uses ADAM [31], a gradient-based optimization technique, with a meta-learning rate of 10^{-3} .

In the meta-optimization phase, this gradient-based optimizer differentiates through the unrolled computational graph of the adaptation phase. Thus, the non-linear layers are double differentiated, once to compute e_L (Eq. 4) and a second time by the meta-optimizer. This arrangement will only allow a two-times differentiable non-linear layer, which prohibits using the Rectified Linear Unit, ReLU, as the activation function σ . Instead, we use the softplus function (Eq. 11), a continuous, twice-differentiable approximation of the ReLU function. In Eq. 11, parameter β controls the smoothness of the function.

In the present examples, each task contains $M = 5$ labels. Consequently, assembling a diverse set of 5-way classification tasks requires a database with a large number of classes. Thus, databases such as MNIST [23], which only has ten classes, are unsuitable for proper meta-training. On the other hand, in each episode, the classifier $f_{\mathbf{w}}$ is reinitialized with random weights \mathbf{W} . Therefore, the task should contain enough data points per class to train $f_{\mathbf{w}}$ adequately. Hence, databases such as Omniglot [32] with only 20 data points per character designed for few-shot learning (*e.g.*, with meta-optimized \mathbf{W}) are impractical in the present framework. In the current work, meta-training tasks are made from the EMNIST database [33]. This database contains 47 classes, making it a good candidate for the meta-plasticity framework. Each task contains $K = 50$ training and $Q = 10$ query data points per class.

Notably, the use of $K = 50$ training data per class with $M = 5$ classes in each episode means that the metalearned plasticity rule needs to train a randomly initialized network with only 250 training data points. Hence, our models are in a low data regime without the benefit of pre-trained weights that are often used for few-shot learning.

References

- [1] D. E. Rumelhart, G. E. Hinton, and R. J. Williams. Learning representations by back-propagating errors. *nature*, 323(6088):533–536, 1986.
- [2] J. C. Whittington and R. Bogacz. Theories of error back-propagation in the brain. *Trends in cognitive sciences*, 23(3):235–250, 2019.
- [3] T. P. Lillicrap, A. Santoro, L. Marris, C. J. Akerman, and G. Hinton. Backpropagation and the brain. *Nature Reviews Neuroscience*, 21(6):335–346, 2020.
- [4] S. Grossberg. Competitive learning: From interactive activation to adaptive resonance. *Cognitive science*, 11(1):23–63, 1987.
- [5] T. P. Lillicrap, D. Cownden, D. B. Tweed, and C. J. Akerman. Random synaptic feedback weights support error backpropagation for deep learning. *Nature communications*, 7(1):1–10, 2016.
- [6] Y. Amit. Deep learning with asymmetric connections and hebbian updates. *Frontiers in computational neuroscience*, 13:18, 2019.
- [7] S. Bartunov, A. Santoro, B. Richards, L. Marris, G. E. Hinton, and T. Lillicrap. Assessing the scalability of biologically-motivated deep learning algorithms and architectures. *Advances in neural information processing systems*, 31, 2018.
- [8] A. Nøkland. Direct feedback alignment provides learning in deep neural networks. *Advances in neural information processing systems*, 29, 2016.
- [9] Q. Liao, J. Leibo, and T. Poggio. How important is weight symmetry in backpropagation? In *Proceedings of the AAAI Conference on Artificial Intelligence*, volume 30, pages 1837–1844, 2016.
- [10] S. Ioffe and C. Szegedy. Batch normalization: Accelerating deep network training by reducing internal covariate shift. In *International conference on machine learning*, pages 448–456. PMLR, 2015.
- [11] M. Akrouf, C. Wilson, P. Humphreys, T. Lillicrap, and D. B. Tweed. Deep learning without weight transport. *Advances in neural information processing systems*, 32, 2019.
- [12] D. O. Hebb. *The organization of behavior: A neuropsychological theory*. Psychology Press, 2005.
- [13] D. Kounin, A. Nayebi, J. Sagastuy-Brena, S. Ganguli, J. Bloom, and D. Yamins. Two routes to scalable credit assignment without weight symmetry. In *International Conference on Machine Learning*, pages 5511–5521. PMLR, 2020.
- [14] J. Schmidhuber. Learning to control fast-weight memories: An alternative to dynamic recurrent networks. *Neural Computation*, 4(1):131–139, 1992.

- [15] C. Finn, P. Abbeel, and S. Levine. Model-agnostic meta-learning for fast adaptation of deep networks. In *International conference on machine learning*, pages 1126–1135. PMLR, 2017.
- [16] K. Javed and M. White. Meta-learning representations for continual learning. *Advances in Neural Information Processing Systems*, 32, 2019.
- [17] J. Lindsey and A. Litwin-Kumar. Learning to learn with feedback and local plasticity. *Advances in Neural Information Processing Systems*, 33:21213–21223, 2020.
- [18] E. Oja. Simplified neuron model as a principal component analyzer. *Journal of mathematical biology*, 15(3):267–273, 1982.
- [19] T. Miconi, K. Stanley, and J. Clune. Differentiable plasticity: training plastic neural networks with backpropagation. In *International Conference on Machine Learning*, pages 3559–3568. PMLR, 2018.
- [20] T. Miconi, A. Rawal, J. Clune, and K. O. Stanley. Backpropamine: training self-modifying neural networks with differentiable neuromodulated plasticity. In *International Conference on Learning Representations*, 2018.
- [21] S. Bengio, Y. Bengio, and J. Cloutier. On the search for new learning rules for anns. *Neural Processing Letters*, 2(4):26–30, 1995.
- [22] B. Confavreux, F. Zenke, E. Agnes, T. Lillicrap, and T. Vogels. A meta-learning approach to (re) discover plasticity rules that carve a desired function into a neural network. *Advances in Neural Information Processing Systems*, 33:16398–16408, 2020.
- [23] Y. LeCun, L. Bottou, Y. Bengio, and P. Haffner. Gradient-based learning applied to document recognition. *Proceedings of the IEEE*, 86(11):2278–2324, 1998.
- [24] E. Oja. Data compression, feature extraction, and autoassociation in feedforward neural networks. *Artificial neural networks*, 1991.
- [25] E. Oja. Principal components, minor components, and linear neural networks. *Neural networks*, 5(6):927–935, 1992.
- [26] R. J. Williams. *Feature discovery through error-correction learning*, volume 8501. Institute for Cognitive Science, University of California, San Diego, 1985.
- [27] J. Karhunen and J. Joutsensalo. Representation and separation of signals using nonlinear pca type learning. *Neural networks*, 7(1):113–127, 1994.
- [28] J. Karhunen and J. Joutsensalo. Generalizations of principal component analysis, optimization problems, and neural networks. *Neural Networks*, 8(4):549–562, 1995.
- [29] N. B. Karayiannis. Accelerating the training of feedforward neural networks using generalized hebbian rules for initializing the internal representations. *IEEE transactions on neural networks*, 7(2):419–426, 1996.

- [30] X. Glorot and Y. Bengio. Understanding the difficulty of training deep feedforward neural networks. In *Proceedings of the thirteenth international conference on artificial intelligence and statistics*, pages 249–256. JMLR Workshop and Conference Proceedings, 2010.
- [31] D. P. Kingma and J. Ba. Adam: A method for stochastic optimization. *arXiv preprint arXiv:1412.6980*, 2014.
- [32] B. M. Lake, R. Salakhutdinov, and J. B. Tenenbaum. Human-level concept learning through probabilistic program induction. *Science*, 350(6266):1332–1338, 2015.
- [33] G. Cohen, S. Afshar, J. Tapson, and A. Van Schaik. Emnist: Extending mnist to handwritten letters. In *2017 international joint conference on neural networks (IJCNN)*, pages 2921–2926. IEEE, 2017.

Supplementary Material

Performance of DFA

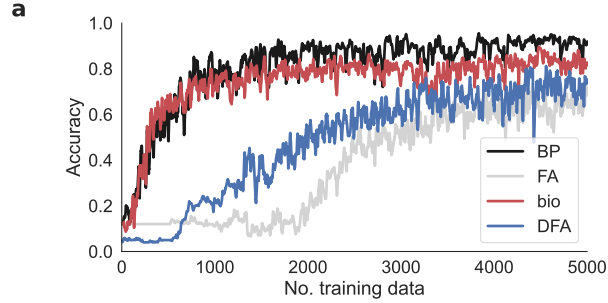


Figure S1: **Performance of benchmark learning schemes** while training a 5-layer fully-connected classifier network on MNIST digits [23]. (a) Accuracy versus the number of training data for Feedback Alignment (FA) [5], Direct Feedback Alignment (DFA) [8], and backprop (BP) [1] methods, compared to the discovered biologically inspired plasticity rule (bio) in Sec. 2.2.2. (b) The angle α_ℓ between the teaching signal e_ℓ^{FA} transmitted by the Feedback Alignment method and the corresponding backpropagated signal e_ℓ^{BP} .

Performance of the \mathcal{F}^{bio}

Fig. S2 demonstrates the classifier’s performance with \mathcal{F}^{bio} within 500 iterations of the meta-optimizer. Comparing the loss and accuracy of \mathcal{F}^{bio} with \mathcal{F}^0 via feedback alignment in Fig. S2a and Fig. S2b, respectively, shows a significant boost in learning through \mathcal{F}^{bio} . Figure S2c further shows improvement in the alignment of the modulating signals with those of the backprop. These angles are reduced the most in the deeper layers. Lastly, Fig. S2d illustrates the progress of the meta-parameters. We observe that the plasticity coefficients converge in about 200 episodes.

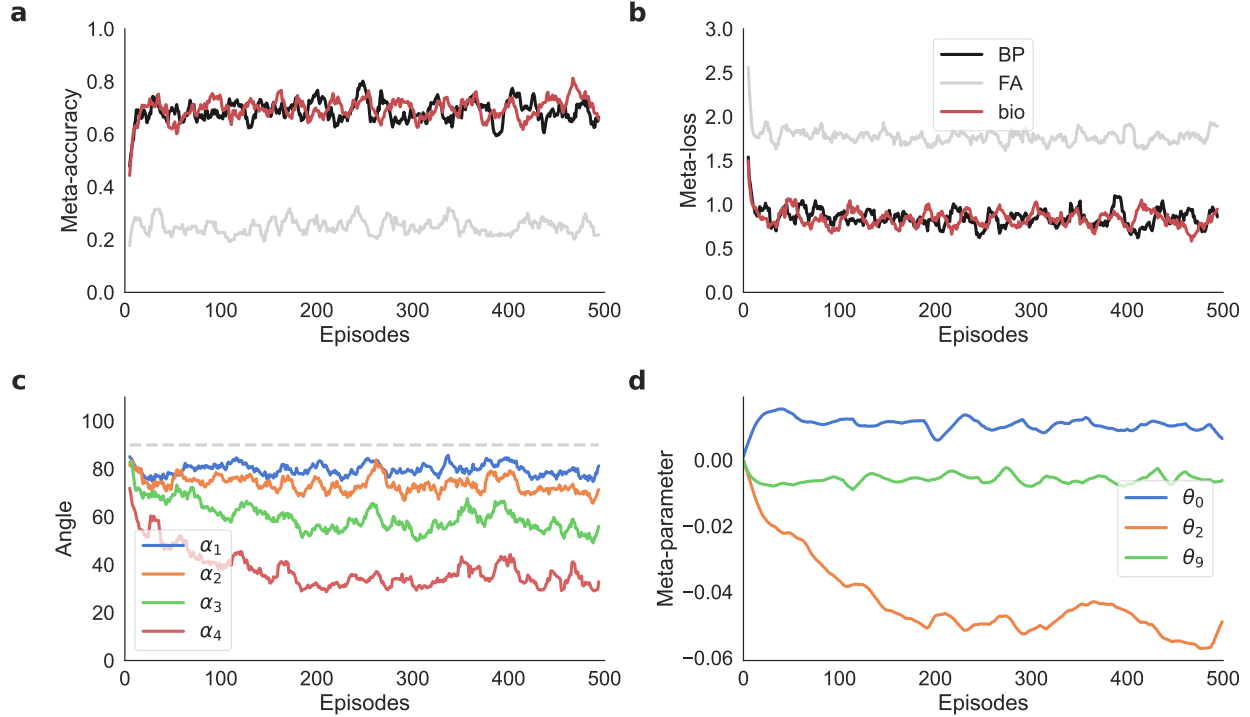


Figure S2: **Performance of the classifier network trained with \mathcal{F}^{bio} plasticity rule:** Comparison between (a) meta-accuracy and (b) meta-loss of \mathcal{F}^{bio} rule with \mathcal{F}^0 via feedback alignment (FA) and backprop (BP), (c) alignment angles between modulating signals of \mathcal{F}^{bio} and backprop, and (d) convergence of the plasticity meta-parameters. While the term \mathcal{F}^{bio} was discovered by regularizing the meta-loss with the penalty term in Eq. 6 (See Methods), λ is set to zero for the illustrations in this figure for the uncovered rule.

Data flow in \mathcal{F}^{eHebb}

Table 1 demonstrates the effect of the Hebbian-like error plasticity term (Eq. 8) on the alignment angles of the modulator signals. Here, we explain these improvements by illustrating \mathcal{F}^{eHebb} 's influence on the feedback pathway's interactions with the forward path. To set the baseline, Fig. S3a employs the plasticity rule

$$\mathcal{F}^0(\Theta) = -\theta_0 \mathbf{e}_\ell \mathbf{y}_{\ell-1}^T \quad (12)$$

to train the network (row 1 in Tab. 1), where \mathbf{e}_ℓ is transmitted through random feedback pathways. First, information from backward connections $\mathbf{B}_{2,1}$ and $\mathbf{B}_{3,2}$ (through $\mathbf{B}_{2,1}$) flows into $\mathbf{W}_{0,1}$ via Eqs. 3 and 12. Similarly, information from $\mathbf{B}_{3,2}$ flows into $\mathbf{W}_{1,2}$ during the weight update. Then in the forward pass, information from $\mathbf{W}_{0,1}$ and $\mathbf{W}_{1,2}$ are propagated forward into $\mathbf{W}_{2,3}$. Table 1 shows that this flow of information does not sufficiently adjust \mathbf{W} for a good alignment of the teaching signals, particularly in online training with limited data.

In Fig. S3b, we add the Hebbian-style error term to update $\mathbf{W}_{2,3}$ using \mathcal{F}^{eHebb} , while the rest of the network is trained with \mathcal{F}^0 through feedback alignment (Tab. 1, row 3). The information flow to $\mathbf{W}_{0,1}$ and $\mathbf{W}_{1,2}$ stays the same; however, \mathcal{F}^{eHebb} introduces an auxiliary information channel from $\mathbf{B}_{3,2}$ to $\mathbf{W}_{2,3}$. As presented in Tab. 1, this supplementary channel results in a better alignment of \mathbf{e}_2 with the corresponding error vector transmitted via backprop.

Figure S3c repeats this experiment with $\mathbf{W}_{1,2}$ updated using \mathcal{F}^{eHebb} while other layers are updated with \mathcal{F}^0 with feedback alignment (Tab. 1, row 2). Although $\mathbf{W}_{0,1}$ is updated with the

same flow of information as Fig. S3b, there is a new flow from $\mathbf{B}_{2,1}$ to $\mathbf{W}_{1,2}$, which improves \mathbf{e}_1 's alignment. Note that better alignment of \mathbf{e}_1 results in more backprop-like weight update, which subsequently improves data propagation to the downstream layers. As a result, the alignments in the downstream layers are slightly improved as well, even with the vanilla \mathcal{F}^0 plasticity rule with feedback alignment updating them. This behavior is similar to the reduced alignment angles in Fig. 7c, where \mathcal{F}^{Oja} positively affects the alignments by improving the forward data propagation.

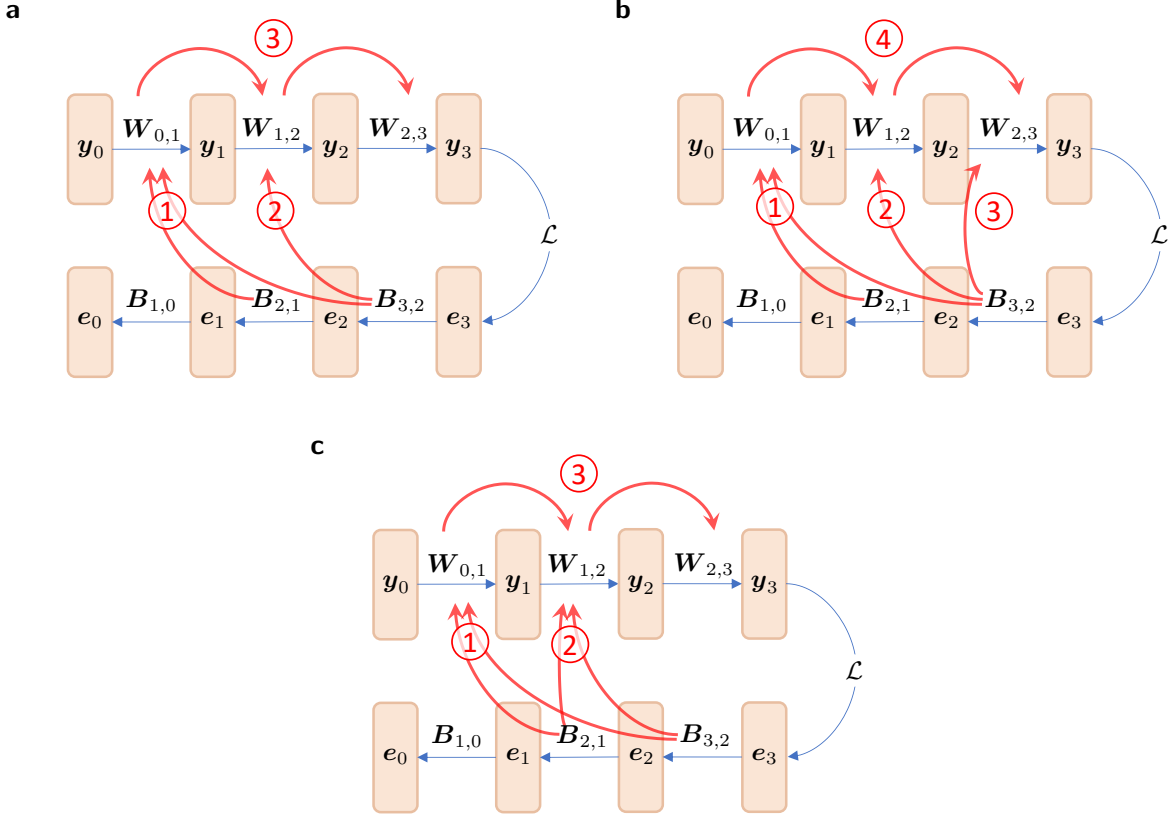


Figure S3: Interactions between feedback and forward pathways using \mathcal{F}^{eHebb} . (a) All layers trained with \mathcal{F}^0 via feedback alignment, (b) $\mathbf{W}_{2,3}$ is updated using \mathcal{F}^{eHebb} , while $\mathbf{W}_{0,1}$ and $\mathbf{W}_{1,2}$ are trained with \mathcal{F}^0 via feedback alignment, (c) $\mathbf{W}_{0,1}$ and $\mathbf{W}_{2,3}$ use \mathcal{F}^0 via feedback alignment, and $\mathbf{W}_{1,2}$ utilizes \mathcal{F}^{eHebb} . In all graphs, blue arrows represent the propagation of data through the forward or backward path, while the red arrow represents the flow of information from the backward pathway to the forward connections.

Expectation of Hebbian-style error-based plasticity

Assume that the entries of $\mathbf{B}_{\ell+1,\ell}$ are i.i.d. with expectation zero and independent from the entries of $\mathbf{e}_{\ell+1}$. Also assume that the entries of \mathbf{e}_ℓ have variance σ_ℓ^2 . In this Supplementary section, we show that

$$\mathbb{E}[\mathbf{e}_\ell \mathbf{e}_{\ell-1}^T \mid \mathbf{B}_{\ell,\ell-1}] = \sigma_\ell^2 \mathbf{B}_{\ell,\ell-1}^T \quad (13)$$

We must first show that $\mathbb{E}[(\mathbf{e}_\ell)_j] = 0$ and $\mathbb{E}[(\mathbf{e}_\ell)_i(\mathbf{e}_\ell)_j] = 0$ when $i \neq j$ by computing

$$\begin{aligned}\mathbb{E}[(\mathbf{e}_\ell)_j] &= \mathbb{E}\left[\left(\sum_k (\mathbf{B}_{\ell+1,\ell})_{j,k} (\mathbf{e}_{\ell+1})_k\right)\right] \\ &= \sum_k \mathbb{E}\left[(\mathbf{B}_{\ell+1,\ell})_{j,k}\right] \mathbb{E}[(\mathbf{e}_{\ell+1})_k] \\ &= 0.\end{aligned}$$

Now, assume that $i \neq j$ and compute

$$\begin{aligned}\mathbb{E}[(\mathbf{e}_\ell)_i(\mathbf{e}_\ell)_j] &= \mathbb{E}\left[\left(\sum_k (\mathbf{B}_{\ell+1,\ell})_{i,k}\right) (\mathbf{e}_{\ell+1})_k \left(\sum_{k'} (\mathbf{B}_{\ell+1,\ell})_{j,k'}\right) (\mathbf{e}_{\ell+1})_{k'}\right] \\ &= \sum_{k,k'} \mathbb{E}\left[(\mathbf{B}_{\ell+1,\ell})_{i,k} (\mathbf{B}_{\ell+1,\ell})_{j,k'}\right] \mathbb{E}[(\mathbf{e}_{\ell+1})_k (\mathbf{e}_{\ell+1})_{k'}] \\ &= 0\end{aligned}$$

where the last line follows from the assumptions that $i \neq j$ and $\mathbf{B}_{\ell+1,\ell}$ has independent entries.

Now we can derive Eq. (13) as follows

$$\begin{aligned}\mathbb{E}\left[(\mathbf{e}_\ell \mathbf{e}_{\ell-1}^T)_{i,k} \mid \mathbf{B}_{\ell,\ell-1}\right] &= \mathbb{E}\left[(\mathbf{e}_\ell \mathbf{e}_\ell^T \mathbf{B}_{\ell,\ell-1}^T)_{i,k} \mid \mathbf{B}_{\ell,\ell-1}\right] \\ &= \mathbb{E}\left[\sum_{j=1}^n (\mathbf{e}_\ell \mathbf{e}_\ell^T)_{i,j} (\mathbf{B}_{\ell,\ell-1}^T)_{j,k} \mid \mathbf{B}_{\ell,\ell-1}\right] \\ &= \sum_{j=1}^n \mathbb{E}\left[(\mathbf{e}_\ell)_i (\mathbf{e}_\ell)_j (\mathbf{B}_{\ell,\ell-1}^T)_{j,k} \mid \mathbf{B}_{\ell,\ell-1}\right] \\ &= \mathbb{E}\left[(\mathbf{e}_\ell)_i (\mathbf{e}_\ell)_i (\mathbf{B}_{\ell,\ell-1}^T)_{i,k} \mid \mathbf{B}_{\ell,\ell-1}\right] \\ &= \sigma_\ell^2 (\mathbf{B}_{\ell,\ell-1}^T)_{i,k}\end{aligned}$$

The last two lines follow from the fact that whenever $i \neq j$, the expectation is equal to zero. Eq. (13) follows directly.